Journal Pre-proof

Mass transfer kinetics of CO$_2$ and eugenol in the supercritical impregnation of polyamide fibers: Experimental data and modeling

José E. Mosquera, María L. Goñi, Raquel E. Martini, Nicolás A. Gañán

Please cite this article as: Mosquera JE, Goñi ML, Martini RE, Gañán NA, Mass transfer kinetics of CO$_2$ and eugenol in the supercritical impregnation of polyamide fibers: Experimental data and modeling, *The Journal of Supercritical Fluids* (2020), doi: https://doi.org/10.1016/j.supflu.2020.105030

Mass transfer kinetics of CO_2 and eugenol in the supercritical impregnation of polyamide fibers: Experimental data and modeling.

José E. Mosquera[a,b], María L. Goñi[a,b], Raquel E. Martini[a,b], Nicolás A. Gañán[a,b,*]

[a]Instituto de Investigación y Desarrollo en Ingeniería de Procesos y Química Aplicada (IPQA-UNC-CONICET), Av. Vélez Sarsfield 1611, X5016GCA, Córdoba, Argentina

[b]Universidad Nacional de Córdoba, Facultad de Ciencias Exactas, Físicas y Naturales, Instituto de Ciencia y Tecnología de los Alimentos (ICTA-FCEFyN-UNC). Av. Vélez Sarsfield 1611, X5016GCA, Córdoba, Argentina

*E-mail address: nicolas.ganan@unc.edu.ar (N.A. Gañán)

GRAPHICAL ABSTRACT
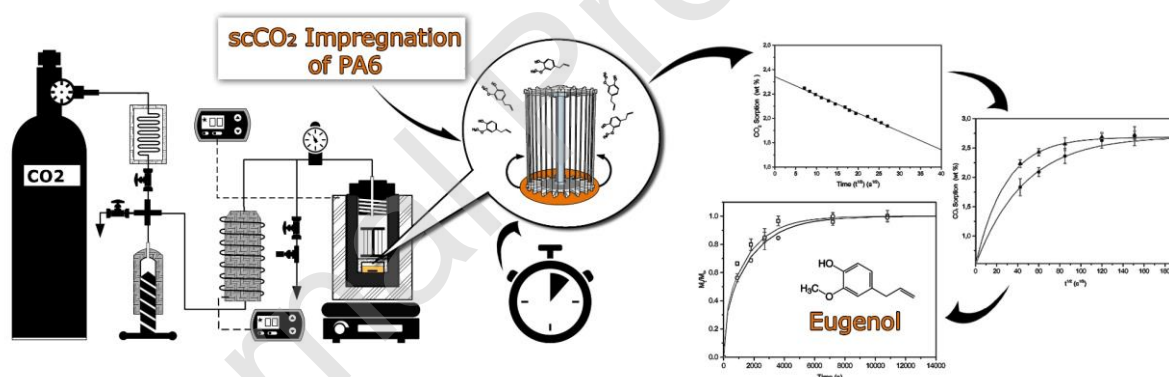
HIGHLIGHTS

- CO_2 and eugenol diffusion in PA6 at supercritical conditions showed Fickian behavior.

- Eugenol loading and partition coefficients were enhanced by temperature.

- Apparent diffusivities of CO_2 and eugenol were approx. 10^{-10} and 10^{-14} $m^2 s^{-1}$, respectively.

- CO_2 sorption in PA6 was not affected by temperature nor pressure.

- Results suggested that eugenol diffuses in an already plasticized polymeric matrix.

- The high pressure process had a low impact on the crystallinity degree of PA6 fibers.

Abstract

In this work, mass transfer kinetics of CO_2 and eugenol into polyamide 6 (PA6) fibers under supercritical conditions were investigated in the context of the development of a functional dental floss for dental care applications using $scCO_2$-assisted impregnation. The sorption kinetics was evaluated at different temperature (40 and 60 °C) and pressure conditions (10 and 12 MPa), measuring the total amount of CO_2 and eugenol incorporated in PA6 fibers after certain time intervals (from 30 min to 4 h). Equilibrium sorption was determined for all operation conditions, obtaining the highest values at low CO_2 density. Diffusion coefficients of CO_2 and eugenol under different process conditions were estimated fitting the experimental data with analytical solutions of the second Fick's law. In addition, thermal behavior of eugenol-loaded PA6 fibers impregnated at different time intervals was evaluated by differential scanning calorimetry (DSC), observing only small changes in the polymer crystallinity during the high-pressure process.

Keywords: Supercritical carbon dioxide, impregnation, polyamide, diffusion coefficient, eugenol.

1. Introduction

2

Supercritical carbon dioxide (scCO$_2$) assisted impregnation has been proposed as an interesting and effective technology to incorporate active substances in polymer matrices for different applications. This process makes use of scCO$_2$ as a promoter agent for dispersing an active compound or additive into a polymeric material [1]. This technology offers several advantages compared to conventional incorporation methods for the development of active materials: it is possible to work at relatively mild conditions due to CO$_2$ low critical point (T_c = 31.4 °C; P_c = 7.38 MPa); scCO$_2$ presents suitable and interesting properties as a solvent, such as low viscosity and surface tension, and a high diffusivity; it is also odorless, colorless, inert, non-toxic, non-flammable, and inexpensive; and it yields solvent-free products after depressurization [2]. scCO$_2$-assisted impregnation allows the incorporation of different types of organic solutes, mainly hydrophobic and thermosensitive compounds (such as many drugs or essential oils) into numerous natural and synthetic polymers based on the plasticizing/swelling effect of CO$_2$ [3]. Due to its several advantages, this technology has been widely studied for the development of active food packaging [4–6], pharmaceutical drug delivery systems [7–10], disposable medical devices [11], active cellulosic products [12] and textile dyeing [13–15], among other applications. In some cases, such as supercritical dyeing, it has been successfully applied at an industrial scale [16].

The knowledge of the mass transfer characteristics of small molecules in polymeric materials is of fundamental importance for the understanding, design, and optimization of supercritical impregnation processes, since it can provide information about the expected duration of the treatment, depending on the operative conditions, and how it can be efficiently reduced. In fact, the solute diffusion in the swollen polymeric matrix is usually the rate-limiting step of the whole process. Diffusion coefficient (D) is a measure of the mobility of a species in a medium [17] and is one of the most important kinetic parameters used to evaluate barrier properties and performance of polymeric materials in a wide range of applications [18]. Experimental characterization of mass transfer in polymers under scCO$_2$ conditions is a difficult task that often requires specific equipment, robust methods, good quality data, and appropriate models. For this reason, the available data in the open literature are limited, compared to the studies concerning the diffusion at ambient

conditions [6,19]. Different methodologies have been applied to the determination of impregnation diffusion coefficients. For instance, Fleming et al. [1] have applied an in-situ confocal Raman microscopy technique to evaluate the diffusion of a dye (Disperse Red 1) in polyethylene terephthalate (PET) under $scCO_2$ conditions. Other authors, like Kim et al. [20], have proposed a $scCO_2$ extraction-based methodology for determining the diffusion coefficient of dye molecules in polyester. Sicardi et al. [15] have studied the diffusivity of dyes in PET films using a film-roll impregnation method, where diffusion coefficients are estimated from concentration-distance (or penetration) curves at given impregnation times. This method was more recently applied by Goñi et al. [21] for the estimation of the diffusion coefficient of R-(–)-carvone in $scCO_2$-swollen LDPE.

In this context, diffusion of small penetrants in rubbery polymers is often modeled assuming a Fickian behavior, because of its simplicity and mathematical tractability. This approach has been successfully applied in the modeling of sorption and diffusion of $scCO_2$ in various types of polymers [22–28]. Moreover, It is also interesting to note that CO_2 absorption under high-pressure conditions can induce a depression of the polymer glass transition temperature (T_g) even below the impregnation temperature [29], in which case solute diffusion occurs in a transitorily rubbery polymer under Fickian-type conditions.

For this reason, the knowledge of CO_2 solubility and diffusivity into a polymer matrix is also of great importance for the impregnation process, due to the possibility of modifying its morphological and diffusional properties by $scCO_2$-induced swelling and plasticization [30]. Moreover, the actual basis of $scCO_2$-assisted impregnation is the diffusion enhancement that can be achieved by the free volume increase associated with this swelling effect [1]. The occurrence of specific interactions between carbon dioxide and a polymer determines the mass of fluid absorbed into it and its sorption kinetics, which depends also on the pressure and temperature conditions [24]. Several methods and experimental setups have been proposed to measure CO_2–sorption kinetics in polymers. According to the literature data, the most commonly used techniques are the transmission IR spectroscopy method [31], the quartz crystal microbalance method [32], and the gravimetric desorption method. This latter procedure was proposed by Berens et al. [33] and does not require specific analytical

equipment. It consists of exposing a sample to $scCO_2$ during a certain time and after a rapid decompression, transfer it to a precision balance and record the weight loss by CO_2 desorption along time. A simple backward extrapolation gives the amount of CO_2 initially sorbed in the sample [33]. Several studies have focused on the sorption and diffusional properties of $scCO_2$ in different types of polymer, such as polyethylene terephthalate (PET) [34], poly(butylene adipate-co-terephthalate) (PBAT) [35], poly chlorotrifluoroethylene (PCTFE)[28], poly(vinyl acetate) and polystyrene [36], polyamide 11 [37], polysulfone [38], polycarbonate [39], poly(l-lactic acid) (PLLA) [24], and poly(methyl methacrylate) (PMMA) [40].

In this work, the CO_2 sorption kinetics in polyamide (PA) fibers and their $scCO_2$-assisted impregnation with eugenol as an active compound are studied. In a previous contribution [41] $scCO_2$-assisted impregnation was evaluated for obtaining an active floss suitable for dental care applications by loading PA fibers with eugenol at 60 °C and different pressure levels and depressurization rates, analyzing the effect of these variables on the impregnation yield. In addition to confirming the feasibility of the process, with loading results up to 15% wt., it was also observed that the high-pressure treatment did not significantly affect the mechanical behavior of the material. The release kinetics of eugenol from impregnated fibers to air and artificial saliva were also studied and modeled, obtaining estimated apparent diffusion coefficients of $1.70 - 2.55 \times 10^{-14}$ m^2 s^{-1} in air and $1-2 \times 10^{-14}$ m^2 s^{-1} in artificial saliva. Moreover, in vitro antimicrobial activity of the impregnated floss against *Escherichia coli* and *Staphylococcus aureus* was confirmed.

Nevertheless, to the best of our knowledge, there are no reports of solubility and diffusion data of eugenol and CO_2 in PA in the open literature. Therefore, this contribution aims to investigate the $scCO_2$ sorption and eugenol impregnation kinetics in PA6 at different operation conditions, estimating the apparent diffusion coefficients of both species in this polymer.

2. Materials and methods

2.1. Materials

A commercial dental floss made of polyamide 6 (PA6, 86.97 ± 0.73 mg·m^{-1}, BucalTac Dental Care, Argentina), composed of approx. 130 filaments of 24.7 ± 11 μm diameter each, was used as a polymer matrix in the impregnation tests. Eugenol (purity: 99%, MW: 164.2 g·mol^{-1}, bp: 254 °C) was purchased from Sigma-Aldrich (USA), and industrial extra-dry carbon dioxide (water content ≤ 10 ppm v/v) from Linde (Argentina). Ethanol (96% v/v, food-grade, Porta, Argentina) was used in the characterization tests. Formic acid (85%, Cicarelli, Argentina) and acetone (Biopack, Argentina) were used as solvents for film casting.

2.2. Film preparation

For CO_2 sorption measurements, polymeric films were prepared in order to obtain specimens of suitable weight and dimensions for this assay. For this purpose, approx. 1 g of dental floss was dissolved into 10 ml of a formic acid: acetone solution (60:40, V/V). Then, the polymer solution was poured into a glass Petri dish (90 mm diameter) and left to dry in a fume hood for 24 h, until it reached a constant weight. After that, a thin film was obtained which was folded, melted, and molded in an automatic flat hot stamping machine (Hex Max, model 3838, Argentina). The final film was cut into strips of 470 ± 10 μm of thickness and an approximate weight of 400 mg.

2.3 CO_2 sorption experiments

CO_2 sorption experiments in PA6 films were performed according to the gravimetric methodology proposed by Berens et al. [33]. The assays were carried out in batch mode using high-pressure equipment schematically presented in Fig. 1. Briefly, the system is composed of a stainless-steel vessel (50 ml of internal volume) (10) with an electrical heating jacket (9) connected to a temperature controller (6) and a magnetic stirrer (8) set at 600 rpm. This cell is provided with a CO_2 cylinder (1), a water-cooling bath (2), and a manual pressure generator in which CO_2 is compressed up to the desired pressure with a pressure generator (3). Before

entering the cell, the CO_2 is pre-heated to the operation temperature through an electrically heated coil (4) that is connected to a temperature controller (5). Finally, the system includes a micrometering valve (7), which allows controlling the depressurization rate. The assays were done at two temperature values (40 and 60 °C) and two pressure values (10 and 12 MPa) during different time intervals (from 30 min to 4 h) under a constant agitation rate (600 rpm). In each run, a film sample was placed inside the cell using a metallic mesh support (11), which maintains it in a vertical position and fully exposed to the CO_2. After closing and pressurization of the cell, the system was kept under the selected operating conditions during a certain time. Then, after the sorption period, the cell was quickly depressurized (within 20 s), opened, and the sample was immediately weighed in an analytical balance (± 0.0001 g). This step took about one minute or less for each experiment. Weight changes in the polymer sample during CO_2 desorption at atmospheric pressure were recorded at different time intervals starting from the depressurization (t=0). During the first part of the desorption process, the weight loss is approximately linear if represented vs. the square root of time, and therefore the initial mass of CO_2 absorbed at t=0 was estimated at the *y*-intercept obtained by linear extrapolation, as proposed by Berens et al. [33]. This strategy was used to calculate the total amount of CO_2 absorbed by the films at all experimental conditions. Afterward, cumulative sorption curves were constructed from these data, and the time at which the incorporation of CO_2 in the polymer sample reached the equilibrium sorption (S) was estimated. All experiments were performed in duplicate.

2.4. Supercritical CO_2-assisted impregnation

Supercritical CO_2-assisted impregnation assays were performed in the same high-pressure impregnation apparatus illustrated in Fig. 1, following the procedure described in a previous contribution [41] with slight modifications. For each experiment, a 1 m long PA6 floss sample is placed into the cell using a cylindrical support (12) with a metal mesh in the borders, threading the sample through this mesh (see Fig. 1). Samples were impregnated using a constant eugenol mole fraction of 0.0015 in the fluid phase at two temperature levels (40 and 60 °C), two pressure levels (10 and 12 MPa), and different time intervals (from 15 min

7

to 3 h) before depressurization. All the experiments were performed at a constant depressurization rate of 0.5 MPa min^{-1}, condition at which the maximum eugenol loading is achieved, according to a previous study [41]. The depressurization rate was controlled by measuring at regular intervals the pressure drop with time, using a manometer and a chronometer, and adjusting the CO_2 outflow with a micrometering valve accordingly. The amount of eugenol incorporated into the floss samples was determined by ethanol extraction followed by spectrophotometric analysis. The extract absorbance was measured at 280 nm in a UV-visible spectrophotometer (Lambda 25, Perkin Elmer, USA, precision: ± 0.001 nm) using a calibration curve prepared in a concentration range of 0.01 to 0.11 mg ml^{-1} (y = 0,0128x + 0,6306; R^2 = 0.992). Cumulative impregnation curves were constructed until equilibrium (maximum loading) was reached. All experiments were performed in duplicate.

The partition coefficient ($K_{p/f}$) of eugenol between the polymer and the fluid phase was estimated from the ratio of eugenol concentration in the polymer and the fluid (scCO$_2$), both at equilibrium, according to Eq. 1:

$$K_{\frac{p}{f}} = \frac{q_E^p}{q_E^{CO_2}}$$
(1)

where q_E^p is the loaded amount of eugenol per mass of polymer [g$_{(eugenol)}$/g$_{(polymer)}$] and q_E^{CO2} is the mass fraction of eugenol in the supercritical fluid [g$_{(eugenol)}$/g$_{(CO2)}$].

2.5. Differential scanning calorimetry (DSC)

In order to evaluate the possible variation of crystallinity and other thermal properties of PA6 during the high-pressure experiments, differential scanning calorimetry (DSC) measurements were performed in a Discovery DSC equipment (TA Instruments, UK). Thermograms were obtained from impregnated floss samples at various processing times, under a nitrogen atmosphere (N$_2$ flow = 50 ml min^{-1}), heating from 0 to 280 °C and cooling from 280 to 25 °C, both at a rate of 10 °C min $^{-1}$. From the thermograms analysis, the crystallinity degree (X$_{CR}$) was estimated according to Eq.2:

8

$$X_{DSC} = \frac{\Delta H}{\Delta H^*} * 100 \qquad (2)$$

were (ΔH) represents the melting enthalpy of the floss sample calculated from the area under the melting peak, and ΔH^* corresponds to the melting enthalpy of 100% crystalline PA6, which is 230 J g^{-1} [42].

2.6. Mathematical modeling

Experimental results of CO_2 sorption and eugenol impregnation were correlated by two mathematical models based on analytical solutions of the second Fick's law for unsteady-state diffusion in thin slabs and cylindrical fibers, respectively, as reported by Crank [43].

2.6.1. Diffusion model for CO_2 sorption:

The apparent diffusion coefficient D_a of CO_2 into polyamide under high-pressure conditions was determined by fitting the CO_2 sorption curves with the analytical solution of second Fick's law proposed by Crank for unsteady diffusion in a plane sheet, given by Eq. 3.

$$\frac{M_t}{M_\infty} = 1 - \frac{8}{\pi^2} \sum_{n=0}^{\infty} \frac{1}{(2n+1)^2} exp\left[-\frac{(2n+1)^2 \pi^2}{L^2} D_a t\right] \qquad (3)$$

where M_t is the sorbed amount of CO_2 into the sample at time t, M_∞ is the equilibrium amount after infinite time, and L is the sample thickness. Eq. 3 can be simplified by truncating at the first term in the summation for the long-time sorption process (Eq. 4).

$$\frac{M_t}{M_\infty} = 1 - \frac{8}{\pi^2} exp\left[-\frac{D_a t \pi^2}{L^2}\right] \qquad (4)$$

This analytical solution is valid under the following conditions and assumptions: (1) The diffusion process can be considered of Fickian-type; (2) diffusion is unidimensional and occurs in the direction of the film thickness; (3) the apparent diffusion coefficient can be considered constant; (4) the resistance to mass transfer on the fluid phase side is negligible compared to the resistance on the polymer side; (5) thermodynamic equilibrium exists at the polymer-fluid interface; and (6) the polymer film is initially free of CO_2. Considering that polyamide is semicrystalline, and therefore it is not a homogeneous medium, we can only estimate an apparent diffusion coefficient (D_a), where the tortuosity effects and the different diffusion behavior of the amorphous and crystalline domains are lumped.

2.6.2. Diffusion model for eugenol impregnation:

The diffusion kinetics of eugenol into the polymer under high-pressure conditions was evaluated taking into account that the dental floss is composed of several long solid cylindrical filaments (24.7 ± 11 μm diameter), as previously confirmed by scanning electron microscopy [41]. Experimental uptake curves were fitted by an analytical solution of the second Fick's law of diffusion in a solid cylinder under non-steady state conditions (Eq. 5) [43]:

$$\frac{M_t}{M_\infty} = 1 - \sum_{n=1}^{\infty} \frac{4}{a^2 \alpha_n^2} \exp(-D_a \alpha_n^2 t) \tag{5}$$

where M_t is the amount of eugenol in the fibers at time t, M_∞ is the total mass of eugenol absorbed, a is the radius of the fiber, D_a is the apparent diffusion coefficient of eugenol in the swollen fiber, and the α_n are the roots of Eq. 5:

$$J_0(a\alpha_n) = 0 \tag{6}$$

where $J_0(x)$ is the Bessel function of the first kind of order zero.

Eq. 5 is valid under the same conditions as Eq. 4, considering in this case diffusion occurring in the radial direction (the fiber radius is much smaller than its length).

2.7. Data fitting

The apparent diffusion coefficients for both models were obtained by adjusting the experimental impregnation or sorption curves using the least-squares method from Microsoft Excel Solver. The model deviation was estimated as the average absolute relative deviation (AARD%) defined according to Eq. (7).

$$AARD\% = \frac{1}{N}\sum_{i=1}^{N}\frac{|x_{i,exp}-x_{i,calc}|}{x_{i,exp}} \times 100 \tag{7}$$

where $x_{i,exp}$ and $x_{i,calc}$ are the experimental and calculated data, respectively, and N is the number of data points.

3. Results and discussion

3.1. CO_2 Sorption kinetics

The sorption kinetics of CO_2 in PA6 was studied from high-pressure experiments, recording the mass of CO_2 gained by a polymer slab as a function of exposure time at various combinations of pressure and temperature, as explained in Section 2.3. Fig. 2 shows an example of a CO_2 desorption curve, where the sorption value (before depressurization) is determined by linear regression and taking the y-intercept. Table 1 reports the CO_2 equilibrium sorption values and the estimated apparent diffusion coefficient for all studied experimental conditions, while Fig. 3 shows representative CO_2 sorption curves. In all cases, equilibrium was reached after approx. 4 h of exposure. As can be seen, pressure and temperature did not have a significant effect on the maximum sorption degree, being around ~3 wt.% for all conditions. Martinache et al. [37] have measured the absorption of CO_2 in molten PA11, reporting a value of 4.7 wt % at 10.3 MPa and 215°C. Although the tested

conditions are different, this might suggest a somewhat poor affinity of this type of polymer and CO_2 at high-pressure conditions.

The D_a values for CO_2 in PA6, estimated using Eq. 4, have an order of magnitude of 10^{-10} m^2 s^{-1}, with an AARD < 2%, which indicates that diffusion of CO_2 in PA6 follows a Fickian-type behavior. Note that diffusivities have been assumed constant (i.e., concentration-independent) in all cases, which is supported by the observed low sorption values. It can be seen from Table 1 that D_a decreases with temperature at a given pressure, being this effect more pronounced at 10 MPa ($\sim$ 60% decrease) than at 12 MPa ($\sim$ 20% decrease). This behavior can be related to the effect of temperature and pressure on CO_2 density, which superimposes to the expected increase in diffusivity with temperature. In fact, at a given pressure, CO_2 density decreases with temperature, with a consequent decrease in swelling ability. Therefore, the observed trend is the result of the compromise between these two opposite effects. In our case, the effect of temperature on CO_2 density seems to prevail. A similar phenomenon was also observed by Azimi et al. [44] in styrene-methylmetacrylate copolymers. Other authors have reported an increase in CO_2 sorption diffusivity with temperature in different polymers, such as polycarbonate (PC)[39], poly(vinyl chloride) (PVC) [23] and polysulphone[38], among others. In these cases, experiments were performed in a higher range of pressure (20-40 MPa), where CO_2 density variations are much lower, and therefore the effect of temperature on molecular motion (i.e., increased diffusivity) prevails.

In general, the results are comparable with diffusion coefficients estimated using the methodology proposed by Berens et al. [33], reported in the literature for other types of polymers, such as cross-linked PDMS (7.5 × 10^{-10} m^2 s^{-1} at 10,5 MPa and 40°C) [28], PHBV (1–3.5 × 10^{-11} m^2 s^{-1} at 10–20 MPa and 35–40°C) [26], P(MMA- EHA-EGDMA) (0.9–4.1 × 10^{-10} m^2 s^{-1} at 10–20 MPa and 35–48°C)[30], PBAT (3.3–7.5 × 10^{-10} m^2 s^{-1} at 8–18 MPa and 40–80°C) [35], polysulfone (4.2–9.5 × 10^{-12} m^2 s^{-1} at 20–40 MPa and 40–60°C)[38], PC (0.91–3.36 × 10^{-11} m^2 s^{-1} at 20–40 MPa and 40–60°C) [39], PVC (0.7–2.5 × 10^{-11} m^2 s^{-1} at 20–40 MPa and 40–70°C) [23], PET (0.35–5.3 × 10^{-11} m^2 s^{-1} at 25–35 MPa and 80–120°C)[34], PLA (6.39 × 10^{-11} m^2 s^{-1} at 10 MPa and 40°C) [24]. They are also comparable with those obtained using other methodologies, such as quantification of the swelling extent by images in molten

polyamide 11 (5.3×10^{-7} m^2 s^{-1} at 10 MPa and 215°C) [37] and polycaprolactone (PCL) (1.15–2.85×10^{-10} m^2 s^{-1} at 10–30 MPa and 80°C) [45].

3.2. Eugenol impregnation kinetics into the polyamide films

As explained in Section 2.4, the impregnation of PA6 fibers with eugenol was performed under the same experimental conditions as CO_2 sorption. Table 2 shows the partition coefficient ($K_{p/f}$), the apparent diffusion coefficient of eugenol in polyamide under impregnation conditions (D_a), and the maximum eugenol loading (EL%) including the respective pure CO_2 density value at each combination of pressure and temperature. The sorption diffusivity of eugenol into the polyamide fibers was estimated from eugenol uptake curves, an example of which is shown in Fig. 4.

As can be seen, the loading of eugenol into the polymer increases with impregnation time until saturation is achieved, following a typical Fickian behavior. After approx. 2 h of impregnation, the maximum eugenol loading (equilibrium) was reached in all cases. A very good agreement between the experimental and calculated results was obtained (AARD < 3.5%) which indicates that Fick's diffusion model is appropriate for this type of system. From Table 2, it can be noticed that the incorporation of eugenol was enhanced mainly by temperature and moderately by pressure, the loading values of eugenol ranging between 3 and 16 wt.%. The highest loading value at saturation was observed at 12 MPa and 60°C (~16%) and the lowest at 10 MPa and 40°C (~3.8%). This is consistent with the results reported in our previous study [41], where a 15.27 % eugenol loading was observed for the same polymeric fibers at 12 MPa and 60°C (with 0.5 MPa min^{-1} depressurization rate). These high impregnation values can be attributed to the presence of polar functional groups in the structure of PA6 which can interact by hydrogen-bonding with the OH and ether groups of eugenol.

The partition coefficient of the active compound between the polymer and the fluid phase ($K_{p/f}$) shows a slight increase with pressure (at constant temperature), whereas a temperature increment (at constant pressure) induces a more pronounced increase of this coefficient. For example, at 12 MPa, $K_{p/f}$ increases from 11.66 at 40°C to 36.68 at 60°C. A

13

similar trend has been observed by Sanchez-Sanchez et al. [46], who reported an increment of partition coefficient of mangiferin and iriflophenones (major mango polyphenols) with temperature and pressure in the $scCO_2$-assisted impregnation of mango leaf extracts into a polyester textile. On one hand, CO_2 density and solvent power decrease with temperature, which displaces the partition equilibrium toward the polymer phase. In this way, the highest values of eugenol loading, and partition coefficient were obtained at low CO_2 density (below $\sim$500 kg m^{-3}). Moreover, temperature enhances the polymer plasticization [20], which favors the penetration and incorporation of eugenol molecules and the interaction between their polar functional groups with the polymer chains. On the other hand, pressure effects are mainly related to the swelling of the polymer induced by CO_2 sorption. In this sense, the limited dependence of $K_{p/f}$ with pressure (at constant temperature) is in agreement with the nearly constant sorption values reported above (Section 3.1).

The apparent diffusion coefficient of eugenol into the polyamide was estimated from experimental impregnation kinetics data by fitting Eq. (5). From Table 2 it can be noticed that the diffusion coefficient ranged between 1.21×10^{-14} and 1.51×10^{-14} m^2 s^{-1}. These data suggest that D_a values are practically independent of pressure and temperature within this range of conditions. This behavior can be related to the CO_2 sorption process, taking into account that the impregnation involves a ternary (CO_2-eugenol-polymer) system. The key feature in $scCO_2$-assisted impregnation is the diffusion enhancement produced by CO_2 sorption, that swells the polymeric matrix, increasing its free volume and its diffusional properties, thus allowing a faster diffusion of other solute molecules [33,47]. Therefore, it is expected that a higher sorption degree will induce a faster impregnation. As seen in Section 3.1, the amount of CO_2 sorbed by PA6 was practically constant at all studied conditions, and therefore a similar eugenol diffusivity in the polymer matrix seems expectable.

On the other hand, the eugenol diffusion coefficient under impregnation conditions is one order of magnitude higher (10^{-14} m^2 s^{-1}) than the value obtained at ambient pressure conditions from the release kinetics to the air (10^{-15} m^2 s^{-1}), as reported in our previous study [41]. This also indicates the mass transfer enhancement achieved when the polymer is exposed to a $scCO_2$ atmosphere.

14

It can also be observed that the diffusion coefficient of CO_2 estimated from sorption experiments is four orders of magnitude higher than that of eugenol into PA6 obtained from impregnation under the same experimental conditions (10^{-10} vs 10^{-14} m^2 s^{-1}). In the impregnation context, this indicates that PA6 fibers are rapidly swollen and saturated with CO_2, and therefore eugenol can be considered as diffusing in an already plasticized polymeric matrix. In other words, CO_2 and eugenol diffusion can be decoupled, confirming the validity of the applied model, which assumes single species diffusion and a constant diffusivity along the process.

Although scCO$_2$-assisted impregnation has been studied by many authors, there are relatively little data on the diffusion coefficient values of additives or active substances in CO_2-swollen polymers. For example, Kim et al., [20] evaluated the diffusive behavior of dye molecules in polyester fibers under different scCO$_2$ impregnation conditions, obtaining diffusion coefficients ranging from 0.8×10^{-16} to 8×10^{-16} m^2 s^{-1} (at 25 MPa and 120°C). Fleming et al. [48] reported values for the diffusion coefficients of dyes in PET films under scCO$_2$ atmosphere of $6.75 \pm 1.01 \times 10^{-14}$ m^2 s^{-1} (at 20 MPa and 80°C) using Raman microscopy data, whereas Goñi et al. [21], reported diffusion coefficients of carvone into scCO$_2$-swollen LDPE in the range of 6.5×10^{-11} to 3×10^{-10} m^2 s^{-1} (at 7–9.7 MPa and 35–60°C). The observed variability let to conclude that diffusion coefficient values are highly dependent on the polymer nature and characteristics (percentage of crystallinity, glassy or rubbery state), as well as the CO_2 sorption and swelling ability and the different specific interactions that can occur between functional groups of the polymer and diffusing molecules.

3.3. Thermal analysis

DSC analysis was carried out to investigate the effect of the impregnation time on the thermal behavior of PA6 fibers. The main thermal properties of the original floss and impregnated samples corresponding to different contact times are reported in Table 3. Fig. 5 shows typical DSC thermograms of the original and an impregnated sample. In both curves, two shallow endothermic peaks are observed in the first stage: the first peak (at 50-60°C) can be attributed to dehydration of the polymer [45,49], while the second peak (~75°C) could be related to the polymer transition temperature (T_g), which can be usually found at

15

this temperature [42], although this cannot be assured due to the curve behavior. The third main feature is the sharp endothermic peak at around 217°C, corresponding to the polymer melting point. It can be seen that these temperatures are not affected by the impregnation process. From Table 3, a decrease of approx. 8% in crystallinity can be observed in the impregnated samples, compared to the original material, while the crystallinity variation among treated samples does not exceed 3%, independently of impregnation time. This small structural changes should not have a significant impact on the determination of the diffusion coefficient because these modifications take place in fast time, therefore the characteristics of the matrix are not seriously affected over time, supporting the idea that the polymer is quickly swollen and plasticized by the CO_2 suggesting a simple diffusion of eugenol into the flexible matrix previously modified. Additionally, this confirms that the high-pressure treatment had a negligible impact on the thermal properties of the polymer, and this may also be in agreement with the minor effect of this treatment on the mechanical properties of floss samples reported in our previous study [41].

4. Conclusions

In this contribution, diffusivity phenomena underlying the supercritical impregnation of eugenol into polyamide fibers were investigated in the context of the development of an active floss for dental purposes. The CO_2 sorption kinetics was studied by a gravimetric method, showing that diffusion of CO_2 in PA6 follows a Fickian behavior. Equilibrium sorption values were around 3 wt.%, with negligible effects of temperature and pressure. On the other hand, the incorporation of eugenol was more clearly influenced by temperature and pressure. The eugenol partition coefficient values showed that a higher temperature favors the displacement of the equilibrium towards the polymer phase, enhancing eugenol loading up to approx. 16 wt.%. The impregnation kinetics of PA fibers also showed a Fickian-type behavior. Fitting the experimental data with analytical solutions of second Fick's lay for unsteady diffusion allowed the estimation of the apparent diffusion coefficients of CO_2 and eugenol in PA6. The four-order-of-magnitude difference between their values (10^{-10} m^2/s vs.

16

10^{-14} m^2/s, for CO_2 and eugenol, respectively) indicates that the fiber is rapidly saturated and swollen by CO_2 and therefore eugenol diffusion occurs in an already plasticized medium, justifying the modeling approach as a single-species diffusion. Finally, DSC analysis showed a small decrease in the polymer crystallinity due to the high-pressure treatment, although independent of impregnation time.

Declaration of interests

The authors declare that they have no known competing financial interests or personal relationships that could have appeared to influence the work reported in this paper.

Acknowledgments

REFERENCES

[1]   O.S. Fleming, S.G. Kazarian, Polymer Processing with Supercritical Fluids, Supercrit. Carbon Dioxide Polym. React. Eng. (2006) 205–238.

[2]   P. Girotra, S.K. Singh, K. Nagpal, Supercritical fluid technology: a promising approach in pharmaceutical research., Pharm. Dev. Technol. 18 (2012) 22–38.

[3]   P. Franco, L. Incarnato, I. De Marco, Supercritical CO2 impregnation of α-tocopherol into PET/PP films for active packaging applications, J. CO2 Util. 34 (2019) 266–273.

[4]   S. Milovanovic, G. Hollermann, C. Errenst, J. Pajnik, S. Frerich, S. Kroll, K. Rezwan, J. Ivanovic, Supercritical CO2 impregnation of PLA/PCL films with natural substances for bacterial growth control in food packaging, Food Res. Int. 107 (2018) 486–495.

[5] M.L. Goñi, N.A. Gañán, S.E. Barbosa, M.C. Strumia, R.E. Martini, Supercritical CO2-assisted impregnation of LDPE/sepiolite nanocomposite films with insecticidal terpene ketones: impregnation yield, crystallinity and mechanical properties assessment, J. Supercrit. Fluids. 130 (2017) 337–346.

[6] A. Rojas, A. Torres, F. Martínez, L. Salazar, C. Villegas, M. José Galotto, A. Guarda, J. Romero, Assessment of kinetic release of thymol from LDPE nanocomposites obtained by supercritical impregnation: Effect of depressurization rate and nanoclay content, Eur. Polym. J. 93 (2017) 294–306.

[7] R. Yoganathan, R. Mammucari, N.R. Foster, Impregnation of Ibuprofen into Polycaprolactone using supercritical carbon dioxide, J. Phys. Conf. Ser. 215 (2010) 012087.

[8] Y.A. Hussain, C.S. Grant, Ibuprofen impregnation into submicron polymeric films in supercritical carbon dioxide, J. Supercrit. Fluids. 71 (2012) 127–135.

[9] L.I. Cabezas, I. Gracia, M.T. García, A. De Lucas, J.F. Rodríguez, Production of biodegradable porous scaffolds impregnated with 5-fluorouracil in supercritical CO_2, J. Supercrit. Fluids. 80 (2013) 1–8.

[10] M. Champeau, J.-M. Thomassin, T. Tassaing, C. Jerome, Drug Loading of Sutures by Supercritical CO2 Impregnation: Effect of Polymer/Drug Interactions and Thermal Transitions, Macromol. Mater. Eng. 300 (2015) 596–610.

[11] D.R.C. Pascoal, E.C.M. Cabral-Albuquerque, E.S. Velozo, H.C. de Sousa, S.A.B.V. de Melo, M.E.M. Braga, Copaiba oil-loaded commercial wound dressings using supercritical CO_2: A potential alternative topical antileishmanial treatment, J. Supercrit. Fluids. (2016).

[12] Y. Medina-Gonzalez, S. Camy, J.-S. Condoret, Cellulosic materials as biopolymers and supercritical CO 2 as a green process: chemistry and applications, Int. J. Sustain. Eng. 5 (2012) 47–65.

[13] D. Varga, S. Alkin, P. Gluschitz, B. Peter-Szabó, E. Székely, T. Gamse, Supercritical fluid

dyeing of polycarbonate in carbon dioxide, J. Supercrit. Fluids. 116 (2016) 111–116.

[14] R. Penthala, G. Heo, H. Kim, I. Yeol, E. Hee, Y. Son, Synthesis of azo and anthraquinone dyes and dyeing of nylon-6 , 6 in supercritical carbon dioxide, J. CO2 Util. 38 (2020) 49–58.

[15] A. Ferri, M. Banchero, L. Manna, S. Sicardi, Dye uptake and partition ratio of disperse dyes between a PET yarn and supercritical carbon dioxide, J. Supercrit. Fluids. 37 (2006) 107–114.

[16] H. Zheng, J. Zhang, J. Yan, L. Zheng, An industrial scale multiple supercritical carbon dioxide apparatus and its eco-friendly dyeing production, J. CO2 Util. 16 (2016) 272–281.

[17] J. Siepmann, R. Siegel, M. Rathbone, Fundamentals and Applications of Controlled Release Drug Delivery, Springer, London, 2012.

[18] G. Dhoot, R. Auras, M. Rubino, K. Dolan, H. Soto-Valdez, Determination of eugenol diffusion through LLDPE using FTIR-ATR flow cell and HPLC techniques, Polymer (Guildf). 50 (2009) 1470–1482.

[19] M.L. Goñi, N.A. Gañan, R.E. Martini, M.C. Strumia, Mass transfer kinetics and diffusion coefficient estimation of bioinsecticide terpene ketones in LDPE films obtained by supercritical CO2-assisted impregnation, J. Appl. Polym. Sci. 134 (2017) 45558.

[20] T. Kim, B. Seo, G. Park, Y. Lee, The Journal of Supercritical Fluids Predicting diffusion behavior of disperse dyes in polyester fibers by a method based on extraction, J. Supercrit. Fluids. 157 (2020) 104685.

[21] M.L. Goñi, N.A. Gañán, R.E. Martini, A.E. Andreatta, Carvone-loaded LDPE films for active packaging: Effect of supercritical CO2-assisted impregnation on loading, mechanical and transport properties of the films, J. Supercrit. Fluids. 133 (2018) 278–290.

[22] A.R. Berens, H.B. Hopfenberg, Induction and Measurement of Glassy-State Relaxations

By Vapor Sorption Techniques., J. Polym. Sci. Polym. Phys. Ed. 17 (1979) 1757–1770.

[23] O. Muth, T. Hirth, H. Vogel, Investigation of sorption and diffusion of supercritical carbon dioxide into poly(vinyl chloride), J. Supercrit. Fluids. 19 (2001) 299–306.

[24] J. Yu, C. Tang, Y. Guan, S. Yao, Z. Zhu, Sorption and diffusion behavior of carbon dioxide into poly(l-lactic acid) films at elevated pressures, Chinese J. Chem. Eng. 21 (2013) 1296–1302.

[25] J. Rosolovsky, R.K. Boggess, A.F. Rubíra, L.T. Taylor, D.M. Stoakley, A.K. St. Clair, Supercritical fluid infusion of silver into polyimide films of varying chemical composition, J. Mater. Res. 12 (1997) 3127–3133.

[26] C. Cravo, A.R.C. Duarte, C.M.M. Duarte, Solubility of carbon dioxide in a natural biodegradable polymer: Determination of diffusion coefficients, J. Supercrit. Fluids. 40 (2007) 194–199.

[27] O. Akin, F. Temelli, Effect of supercritical CO_2 pressure on polymer membranes, J. Memb. Sci. 399–400 (2012) 1–10.

[28] K.F. Webb, A.S. Teja, Solubility and diffusion of carbon dioxide in polymers, Fluid Phase Equilib. 158–160 (2002) 1029–1034.

[29] P. Alessi, A. Cortesi, I. Kikic, F. Vecchione, Plasticization of polymers with supercritical carbon dioxide: Experimental determination of glass-transition temperatures, J. Appl. Polym. Sci. 88 (2003) 2189–2193.

[30] A.R.C. Duarte, C. Martins, P. Coimbra, M.H.M. Gil, H.C. de Sousa, C.M.M. Duarte, Sorption and diffusion of dense carbon dioxide in a biocompatible polymer, J. Supercrit. Fluids. 38 (2006) 392–398.

[31] J.R. Fried, W. Li, C. Engineering, High-pressure FTIR Studies of Gas-Polymer Interactions, J. Appl. Polym. Sci. 41 (1990) 1123–1131.

[32] J.H. Aubert, Solubility of carbon dioxide in polymers by the quartz crystal microbalance technique, 11 (1998) 163–172.

[33]   A.R. Berens, G.S. Huvard, R.W. Korsmeyer, F.W. Kunig, Application of compressed carbon dioxide in the incorporation of additives into polymers, J. Appl. Polym. Sci. 46 (1992) 231–242.

[34]   J. von Schnitzler, R. Eggers, Mass transfer in polymers in a supercritical CO2-atmosphere, J. Supercrit. Fluids. 16 (1999) 81–92.

[35]   S. Lin, J. Yang, J. Yan, Y. Zhao, B. Yang, Sorption and diffusion of supercritical carbon dioxide in a biodegradable polymer, J. Macromol. Sci. Part B Phys. 49 (2010) 286–300.

[36]   Y. Sato, T. Takikawa, S. Takishima, H. Masuoka, Solubilities and diffusion coefficients of carbon dioxide in poly(vinyl acetate) and polystyrene, J. Supercrit. Fluids. 19 (2001) 187–198.

[37]   J.D. Martinache, J.R. Royer, S. Siripurapu, F.E. Hénon, J. Genzer, S.A. Khan, R.G. Carbonell, Processing of polyamide 11 with supercritical carbon dioxide, Ind. Eng. Chem. Res. 40 (2001) 5570–5577.

[38]   M. Tang, Y.C. Huang, Y.P. Chen, Sorption and diffusion of supercritical carbon dioxide into polysulfone, J. Appl. Polym. Sci. 94 (2004) 474–482.

[39]   M. Tang, T.B. Du, Y.P. Chen, Sorption and diffusion of supercritical carbon dioxide in polycarbonate, J. Supercrit. Fluids. 28 (2004) 207–218.

[40]   M. Pantoula, C. Panayiotou, Sorption and swelling in glassy polymer/carbon dioxide systems. Part I-Sorption, J. Supercrit. Fluids. 37 (2006) 254–262.

[41]   J.E. Mosquera, M.L. Goñi, R.E. Martini, N.A. Gañán, Supercritical carbon dioxide assisted impregnation of eugenol into polyamide fibers for application as a dental floss, J. CO2 Util. 32 (2019) 259–268.

[42]   T.F. Meyabadi, M.R.M. Mojtahedi, S.A.M. Shoushtari, Melt spinning of reused nylon 6: Structure and physical properties of as-spun, drawn, and textured filaments, J. Text. Inst. 101 (2010) 527–537.

[43]   J. Crank, The mathematics of diffusion, 2nd ed., Oxford University Press, Bristol, 1975.

[44] H.R. Azimi, M. Rezaei, Solubility and diffusivity of carbon dioxide in St-MMA copolymers, J. Chem. Thermodyn. 58 (2013) 279–287.

[45] J. Ivanovic, S. Knauer, A. Fanovich, S. Milovanovic, M. Stamenic, P. Jaeger, I. Zizovic, R. Eggers, Supercritical CO2 sorption kinetics and thymol impregnation of PCL and PCL-HA, J. Supercrit. Fluids. 107 (2016) 486–498.

[46] J. Sanchez-Sanchez, M. Fernández-Ponce, L. Casas, C. Mantell, E.J. Martínez de la Ossa, Impregnation of mango leaf extract into a polyester textile using supercritical carbon dioxide, J. Supercrit. Fluids. 128 (2017) 208–217.

[47] I. Kikic, F. Vecchione, Supercritical impregnation of polymers, Curr. Opin. Solid State Mater. Sci. 7 (2003) 399–405.

[48] O.S. Fleming, F. Stepanek, S.G. Kazarian, Dye diffusion in polymer films subjected to supercritical CO2: Confocal raman microscopy and modelling, Macromol. Chem. Phys. 206 (2005) 1077–1083.

[49] E. Adeli, The use of supercritical anti-solvent (SAS) technique for preparation of Irbesartan-Pluronic® F-127 nanoparticles to improve the drug dissolution, Powder Technol. 298 (2016) 65–72.

Tables

Table 1. Equilibrium sorption (S) and estimated apparent diffusion coefficient (D_a) of CO_2 in PA6.

Pressure (MPa)	Temperature (°C)	S (wt.%)	D_a (m²·s⁻¹)	AARD%
10	40	2.77%	8.00E-10	0.91%
	60	2.81%	4.88E-10	1.51%
12	40	2.87%	6.80E-10	1.94%
	60	2.91%	5.75E-10	1.51%

Results are shown as mean values ± standard deviation (n = 2 replicates).

Table 2. Eugenol loading (EL%), partition coefficient ($K_{p/CO2}$) and estimated apparent diffusion coefficient (D_a) in PA6 fibers.

Pressure (MPa)	Temperature (°C)	CO_2 density (kg m⁻³)[a]	EL%	$K_{p/CO2}$	D_a (m²·s⁻¹)	AARD%
10	40	628.61	3.76%	8.18	1.29E-14	2.0%
	60	289.95	12.56%	30.43	1.21E-14	1.5%
12	40	717.76	5.22%	11.66	1.25E-14	2.7%
	60	434.43	15.96%	36.68	1.51E-14	3.2%

[a] From NIST

Results are shown as mean values ± standard deviation (n = 2 replicates).

Table 3. Thermal properties of eugenol impregnated PA6 fibers (at T = 60°C, P = 12 MPa)

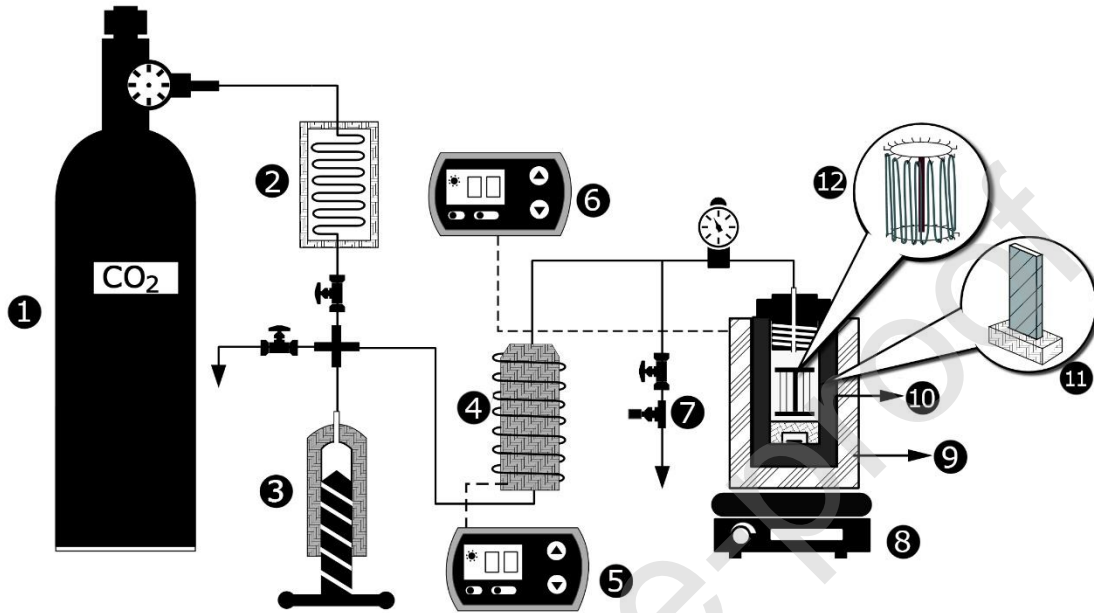| Time (min)	Melting point T_m (°C)	Heat of fusion ΔH_m (J/g)	Crystallinity X_c (%)
0	217.0	66.26	28.00
15	216.0	56.14	24.41
30	217.7	50.45	21.93
45	217.7	53.19	23.12
60	217.0	55.22	24.01
90	217.0	54.87	23.86

Figures

Fig. 1. High pressure impregnation apparatus. 1: CO_2 cylinder; 2: cooling coil; 3: pressure generator; 4: pre-heater; 5, 6: temperature controller; 7: micrometering valve; 8: magnetic stirrer; 9: electrical jacket; 10: high pressure vessel; 11: film sample; 12: dental floss sample.
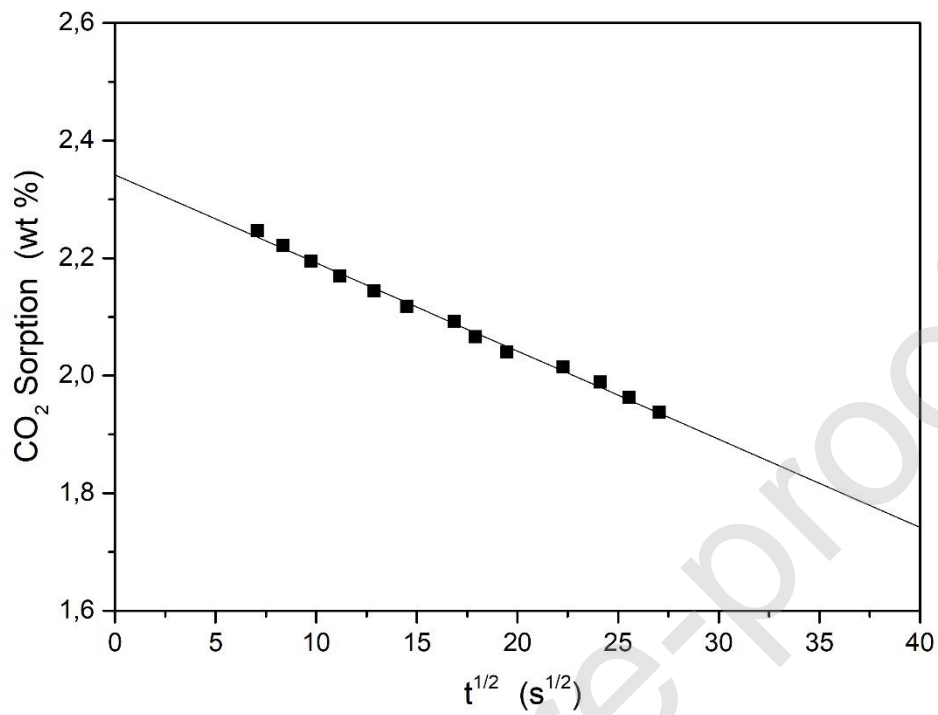
Fig. 2. Example of CO_2 desorption from a polyamide film (450 μm thickness) at P = 10 MPa, T = 60 °C, and a sorption time of 2 h.
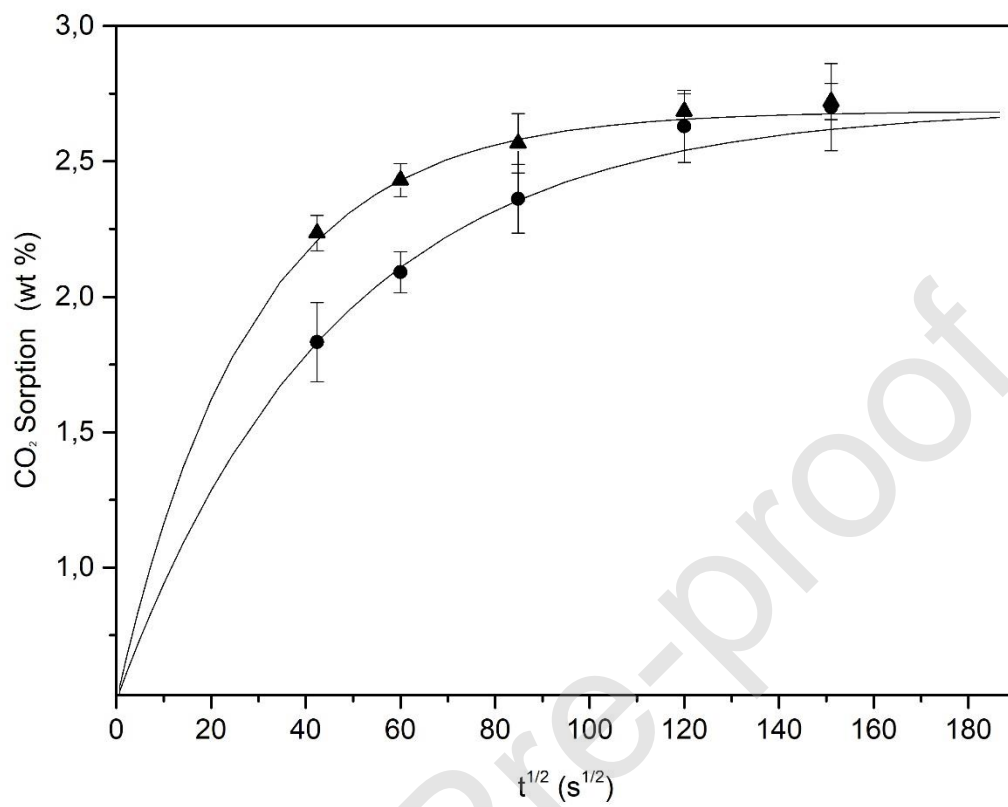
Fig. 3. Example of CO_2 sorption profile into the fibers of polyamide at P = 10 MPa, T = 40 °C (●) and P = 10 MPa, T = 60 °C (▲). Lines: diffusion model correlation. Vertical bars indicate standard deviation (n = 2).
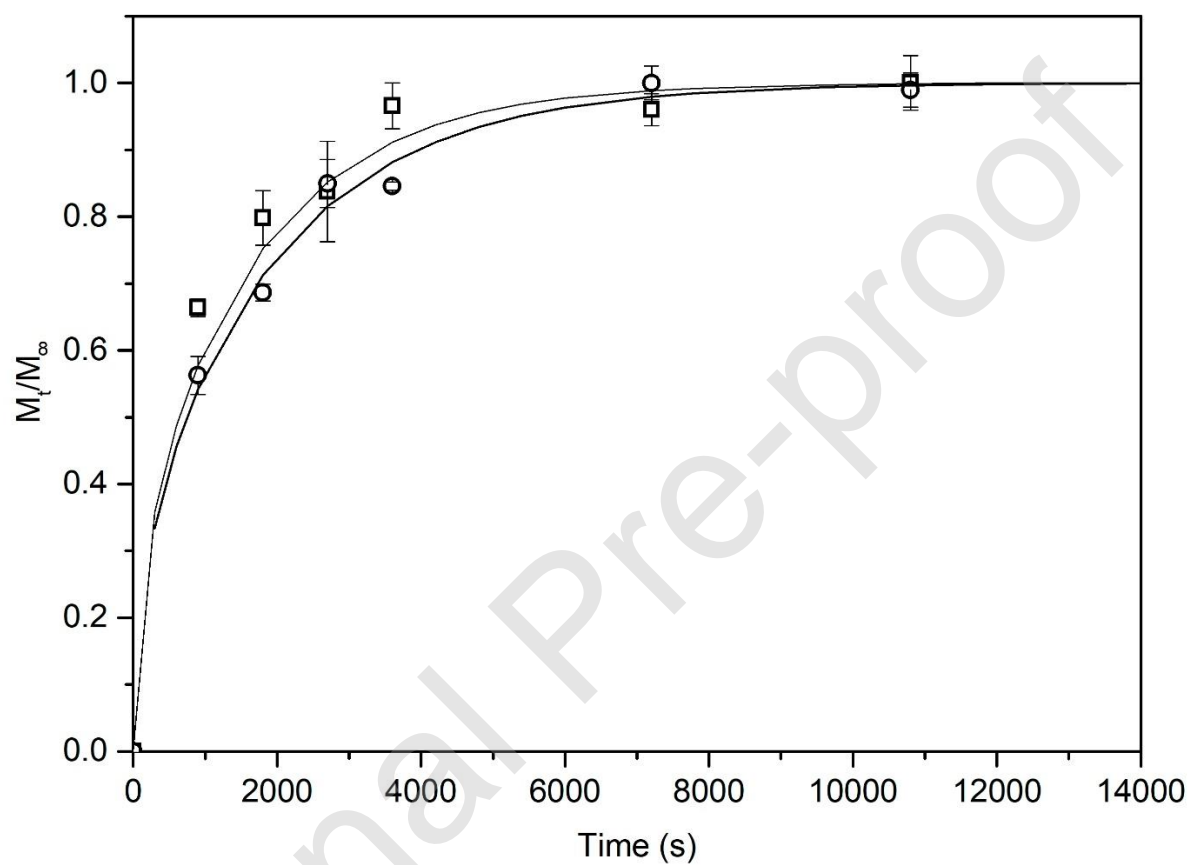
Fig. 4. Example of sorption profile of eugenol into the fibers of polyamide at P = 12 MPa, T = 60 °C (□) and P = 10 MPa, T = 40 °C (○) with depressurization rate of 0.5 MPa min^{-1} for both conditions. Lines: diffusion model correlation. Vertical bars indicate standard deviation (n = 2).
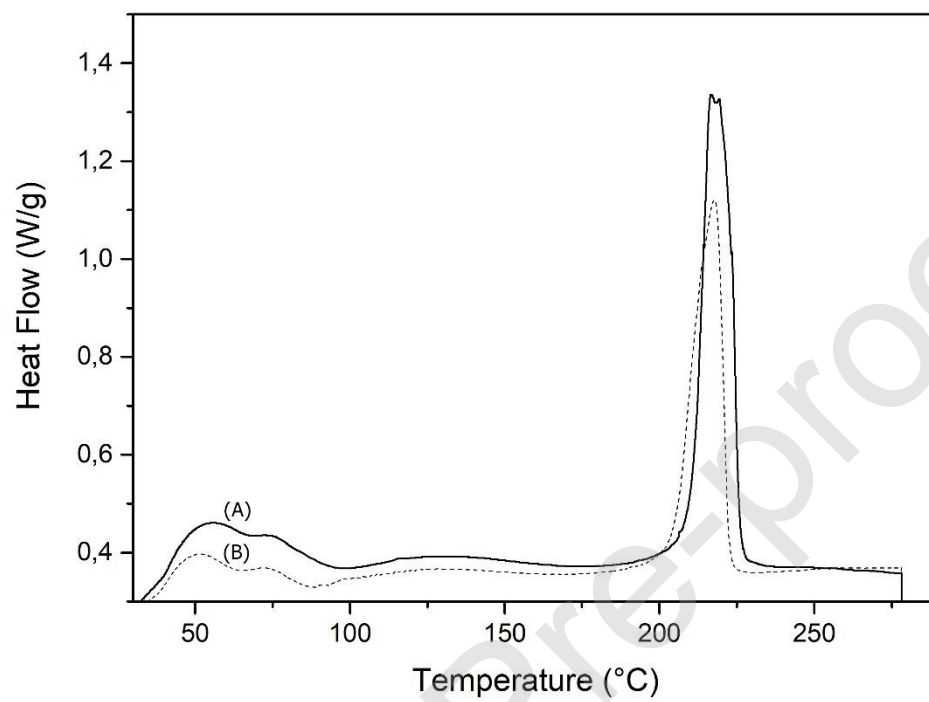
Fig. 5. DSC curves of pure (A) and eugenol-impregnated polyamide fibers at 60 °C and 12 MPa (B).